ChemPubSoc Europe

DOI: 10.1002/cmdc.201900481

CHEMMEDCHEM Full Papers

Oxidative Cyclization-Induced Activation of a Phosphoinositide 3-Kinase Inhibitor for Enhanced Selectivity of Cancer Chemotherapeutics

Haizhou Zhu,[a] Rosalin Mishra,[b] Long Yuan,[b] Safnas F. Abdul Salam,[a] Jing Liu,[a] George Gray,[a] Alyssa D. Sterling,[a] Mark Wunderlich,[c] Julio Landero-Figueroa,[a] Joan T. Garrett,[b] and Edward J. Merino*[a]

In this work, we designed a prodrug that reacts with cellular oxidative equivalents leading to ether cleavage and cyclization to release an active phosphatidylinositol 3-kinase (PI3K) inhibitor. We show that the compound reduces affinity for PI3KA relative to the PI3K inhibitor, is slow to intercellularly oxidize, and is resistant to liver microsomes. We observed modest activity in untreated acute myeloid leukemia cells and 14-fold selectivity relative to non-cancerous cells. The cellular activity of the compound can be modulated by the addition of antioxidants or oxidants, indicating the compound activity is sensitive to cellular reactive oxygen species (ROS) state. Co-treatment with cytosine arabinoside or doxorubicin was used to activate the compound inside cells. We observed strong synergistic activity specifically in acute myeloid leukemia (AML) cancer cells with an increase in selective anticancer activity of up to 90-fold. Thus, these new self-cyclizing compounds can be used to increase the selectivity of anticancer agents.

Introduction

Phosphatidylinositol 3-kinases (PI3Ks) catalyze the phosphorylation of phosphoinositides and are essential for signaling that drives proliferation and metabolic programming.[1] Importantly, PI3K product formation leads to the subsequent activation of serine-threonine kinase AKT and mTOR.[2] Since the PI3K pathway is frequently deregulated in tumors, it is an attractive target for drug development as both a therapeutic and as an adjunct to improve current treatments.[3] Many natural-product PI3K inhibitors, such as wortmannin, have side effects and poor metabolic stability.[4] Side effects result from inhibition of normal homeostatic functions of PI3K, such as metabolic, inflammatory, and memory functions.[5–7] In this work, we focused on a PI3K inhibitor, Pi103, that causes reductions in tumor volume in models of acute myeloid leukemia (AML),[8] lung cancer,[9] and skin cancer but has serious side effects.[10–11] We sought to produce a Pi103 prodrug that improves the specificity and stability of this compound.

Cancer cells have important phenotypic differences compared to normal cells that are exploitable as a prodrug strategy.[12,13] We have designed a prodrug strategy, called self-cyclizing prodrugs, that undergo unique reactions when oxidized specifically in cancer cells, which have high levels of reactive oxygen species (ROS), to produce non-toxic byproducts and release an inhibitor[14–15] (Figure 1). At the biochemical level, ROS are not only deleterious byproducts of metabolism but also serve as signaling molecules. For example, the oxidation of cysteine thiols to disulfides or sulfenic acids leads to altered structure and function of proteins.[16] Alterations in ROS and other oxidative equivalents are critical events in acquired drug

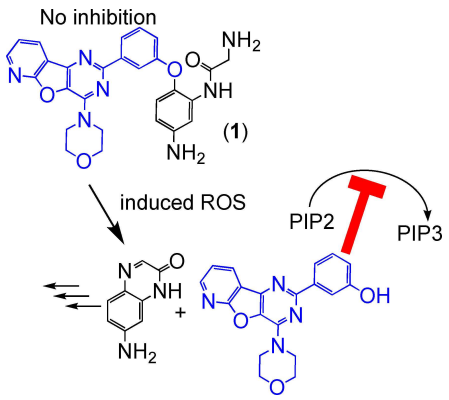

Figure 1. Molecular design of self-cyclizing prodrug. Compound 1 does not bind to PI3Ks. Induction of cellular oxidative equivalents (ROS) causes a tandem reaction leading to cleavage of the ether bond to liberate an active PI3K inhibitor (blue) and self-cyclization products (black).

[a] H. Zhu, S. F. Abdul Salam, J. Liu, G. Gray, A. D. Sterling, Prof. Dr. J. Landero-Figueroa, Prof. Dr. E. J. Merino
Figueroa, Prof. Dr. Edward. J. Merino*
Department of Chemistry, McMicken College of Arts and Sciences
University of Cincinnati
Cincinnati, OH 45221 (USA)
E-mail: merinoed@ucmail.uc.edu
[b] Dr. R. Mishra, L. Yuan, Dr. J. T. Garrett
James L. Winkle College of Pharmacy
University of Cincinnati
Cincinnati, OH 45221 (USA)
[c] Dr. M. Wunderlich
Division of Experimental Hematology and Cancer Biology,
Cincinnati Children's Hospital Medical Center,
Cincinnati, OH 45221 (USA)

Supporting information for this article is available on the WWW under https://doi.org/10.1002/cmdc.201900481

resistance in cancer.[17] For example, it is thought that AKT-induced oxidative equivalents are responsible for the genetic instability and tumor heterogeneity that results in imatinib resistance in AML patients.[18] In addition, common AML oncogenes, like *Ras* and *FLT3*, elevate levels of cellular oxidants.[19–20] Critically, many chemotherapies also induce oxidative equivalents and ROS production; these species can catalyze the activation of self-cyclizing prodrugs to improve selectivity.

Our design of self-cyclizing prodrugs offers advantages that are derived from key observations we have made over time.[21–22] For example, we designed compounds that release antioxidants to protect skin cells in UV-induced high ROS environments. One insight we have found critical, and we have incorporated into this design is to synthesize difficult to oxidize compounds. This design prevents activation in healthy cells that have ROS and likely confers stability to the liver environment. High levels of oxidative stress occur in the tumor microenvironment[23] and during treatment with many chemotherapies (i.e., doxorubicin, cytosine arabinoside). So we propose to make compounds that are activated by large changes in oxidative stress. For comparison, the most common ROS-responsive chemistry utilizes Chan-lam type coupling with an arylboron.[24–27] The activating oxidant is hydrogen peroxide and has shown selectivity in different cancer cell models. While boron-based prodrugs are sensitive to H_2O_2 concentrations their half-lives is in minutes.[28] These boron prodrugs release quinone methides and boron acids that are known to have potential toxicity issues.[29–30] There has been a recent approval of a boron-based drug by the FDA[31] showing ROS-prodrugs can be a viable approach. Thus, we seek alternative designs of oxidation activated compounds. We use a self-cyclizing prodrug strategy to reduce the electrophilic nature of oxidation side products and this manuscript describes our attempt with the Pi103 inhibitor.

This manuscript details the experimental validation of the strategy. We show that **1** (Figure 1) has reduced affinity for target proteins, is slow to release, and can withstand liver microsomes. The reaction pathway inside cells is uncovered and the identified products were independently synthesized and shown to have no to little cell activity. Biological experiments show **1** blocks PI3K activity and is modulated by the status of oxidative stress in the cell. Cancer cell specific synergy is shown in combination with two standard treatments.

Results and Discussion

To design the self-cyclizing Pi103 prodrug, we studied the crystal structure of Pi103 bound to PIK3CA (PDB 4L23); this structure shows the importance the phenol of Pi103[32–33] (Figure 2A). Thus, the phenol of Pi103 was chosen as the point for attachment to the self-cyclizing portion of the molecule to make a ROS-sensitive PI3K prodrug. In compound 1, the 4-hydroxyl of Pi103 and the ROS sensitive portion of the self-cyclizing compound are linked to form an ether that is prone to cleavage under oxidative conditions. Reaction of 1 with ROS is

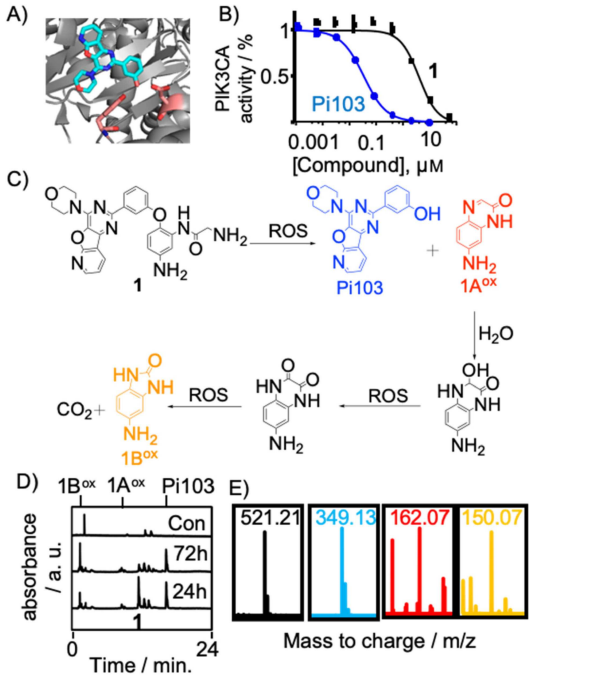

Figure 2. Compound 1 oxidatively releases Pi103. A) View of PI3KCA hydrogen bonds to the phenol of Pi103 (PDB 4L23).[32] B) PI3KCA inhibition by Pi103 (blue) and 1 (black). Error bars are standard deviations from three replicates. C) Oxidative half-reaction of 1 to form Pi103 (blue), $\mathbf{1A}^{ox}$ (red), and $\mathbf{1B}^{ox}$ (yellow). Note that electrons and proton losses are not shown. D) HPLC of extracted Kasumi-1 cell material treated with DMSO (con) or with 5 μM 1 for 24 or 72 h. E) MS spectra of isolated products unique to treatment groups in the HPLC chromatogram. Products were isolate three times and independent MS acquired.

expected to release Pi103 and form a non-cytotoxic aromatic system (black, Figure 2C). Compound 1 was synthesized in three steps, starting from commercially available Pi103, in an overall yield of 60% (Scheme 1). Detailed synthetic procedures, yields, and spectroscopic data including ^{1}H-NMR, ^{13}C-NMR, and high-resolution MS are provided in Supplementary Information.

We first determined the apparent inhibition constant, K_i^{app}, of compound **1** against PI3KCA. PI3KCA was selected since this protein is a known target of Pi103. A previously described luciferase fragment complementation assay was used.[34] In our

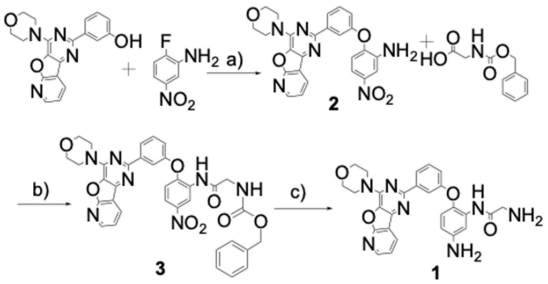

Scheme 1. The synthesis route of compound. **a**) K_2CO_3 in DMF at 70°C, yield: 90%. **b)** 1-[Bis (dimethylamino) methylene]-1H-1,2,3-triazolo[4,5-b]pyridinium 3-oxid hexafluorophosphate in DMF then add diisopropylamine, yield: 40%. **c)**10%Pd/C (10% in w/w) with H_2 (30psi), yield: 95%.

analysis, the K_i^{app} for Pi103 against PI3KCA was 0.031 ± 0.002 μM (Figure 2C), which is similar to the literature value of 0.015 μM. The K_i^{app} of **1** was 0.960 ± 0.08 μM (Figure 2B). Thus, when Pi103 is linked to the self-cyclizing scaffold at the 4-OH position there was about a 30-fold decrease in binding affinity of the inhibitor for PI3KCA. We also performed a 50-kinase activity screen at a 25 μM dose of **1** (Figure S1). None of the kinases were inhibited by more than 85% at this dose.

To verify the proposed mechanism (Figure 2C), we investigated the intracellular oxidation of **1**. In a high ROS environment **1** is oxidized leading the alkylamine to attack and release Pi103. The byproducts are **1**A^{ox} and **1**B^{ox}. Compound **1**B^{ox} derives from **1**A^{ox}. We propose a nucleophilic water attack of the resulting **1**A^{ox} enamine. This reaction generates a compound in an equivalent oxidation state as glyoxylic acid which is known to further oxidize into an oxalate-like state. It is common that oxalate derivative release carbon dioxide (Figure 2C for details) upon oxidation. We examined this proposed pathway within Kasumi-1 cells. Kasumi-1 cells were chosen in this experiment since they are known to possess PI3K-dependent activation of AKT.[35] We treated approximately ten million cells with 5 μM **1** or with DMSO. After 24 or 72 hours, cells were pelleted, incubated in acetonitrile, separated by HPLC, and resulting unique peaks analyzed by MS (Figure 2D). At 24 hours we isolated and obtained MS spectra for **1**, **1**A^{ox}, **1**B^{ox}, and Pi103. Interestingly at 72 hours, the signal for **1** is lost and **1**A^{ox} was reduced to near the detection limit (signal to noise 20 ± 10) with only Pi103 and **1**B^{ox} detected. MS spectra obtained for isolated unique HPLC bands are the proposed products (Figure 2E). These spectra show the M/Z values expected for each compound are the major signals. Oxidation of **1** by peroxide leads to Pi103 formation (Figure S2) as does oxidation by several other types of reactive oxygen species (Figure S3). Although we were not able to isolate the intermediates of the reaction in cells, we were able to identify the intermediates in LCMS analyzed reactions in buffered solutions as shown in Figure S2. These results indicate that 1 is slowly oxidized in cells and that oxidation occurs through the predicted mechanism.

We next examined the effect of **1**, **1**A^{ox}, **1**B^{ox}, and Pi103 on cells using an MTT assay with a 72 hr incubation time. Both **1**A^{ox} and **1**B^{ox} were independently synthesized and experimental spectra are in the supporting information. Figure 3A shows data fitted to a four-parameter sigmoid for the four compounds in Kasumi AML cells while Figure 3B shows data for primary cord blood cells. In Kasumi-1 AML cells the IC_{50} for **1** was 3 ± 1 μM. In contrast, the IC_{50} of 1 in primary cord blood cells from a healthy donor was 43 ± 1 μM. Thus 1 had 14-fold selectivity for the AML cells relative to the normal cells. The difference in activity of **1** likely reflects the differential antioxidant background in the cells (Figure S4). The IC_{50} values of inhibitor alone, Pi103, were similar in the two cell types (0.13 ± 0.05 μM in Kasumi-1 cells and 0.086 ± 0.001 μM in cord blood). The IC_{50} for **1**A^{ox} **1**B^{ox} in both cell types is over 50 μM in both cases, which indicated that cytotoxicity of the **1** is due to release of Pi103 not the cyclization byproduct.

We then examined whether Pi103 released from **1** inhibited PI3K in Kasumi-1 cells. Phosphorylation of serine at position 473 on PI3K substrate AKT was compared to total AKT using an in-cell western in two-color mode.[36] Kasumi-1 cells were treated with **1** or Pi103 (as a positive control) for 24 hours instead of 72 hr incubation. We observed that the ratio of phosphorylated to total AKT decreased in a manner dependent on the concentration of **1** (Figure 3C).

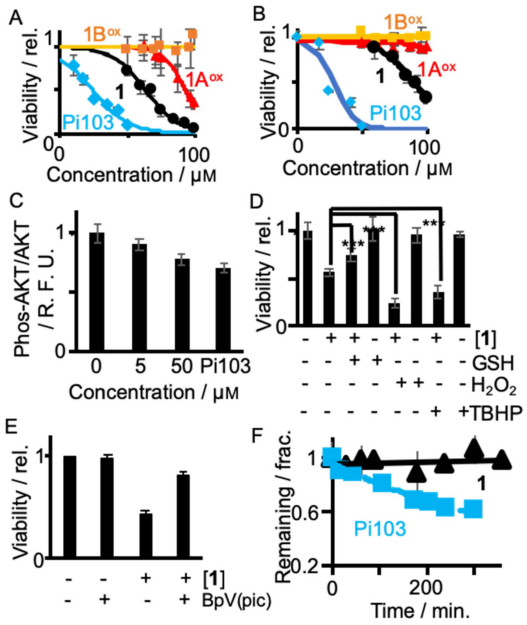

Figure 3. Pi103 released by prodrug **1** effects cancerous but not normal cells. A) Viability of Kasumi-1 cells after 72 hr treatment with **1** (black), Pi103 (blue), and **1**A^{ox} (red), and **1**B^{ox} (yellow). B) Similar data for primary cord blood cells. C) Ratios of phosphorylated AKT to total AKT quantified using in-cell western blot after 24-hr treatment of Kasumi-1 cells with no drug (0), 5 or 50 μM **1**, or 0.15 μM Pi103. D) Treatment of Kasumi-1 cells with the listed reagents for 24 hr and cell viability was determined relative to the untreated control. Concentrations were 5 μM **1**, 100 μM hydrogen peroxide, 100 μM glutathione, or 50 μM tert-butyl hydroperoxide. E) Kasumi-1 cells were treated with 5 μM **1** and/or 1 μM BpV(pic), and cell viability was determined relative to the untreated control. F) Liver microsome stability of **1**, as monitored via HPLC overtime. Analysis of fractions Pi103 (blue) and **1** (black) remaining after incubation with microsomes for the indicated amount of time. All error bars are standard deviations with three replicates. Part C utilized five biological replicates.

The ratio was 0.90 ± 0.01 at 5 μM 1 and 0.77 ± 0.01 at 50 μM **1**. To further establish that self-cyclizing prodrug **1** acts by inhibiting intracellular PI3K, we tested the effect of the PTEN inhibitor BpV(pic), a the bisperoxovanadium derivative. PTEN is a phosphatase that reverses the action of PI3Ks via dephosphorylation of PIP3.[37] Thus if Pi103 released from **1** inhibits PI3K activity, PTEN inhibition should reverse the effect. Although 1 μM BpV(pic) had no effect on the growth of Kasumi cells and 5 μM **1** reduced viability to 42 ± 5%, the combination resulted in 82 ± 3% viability compared to untreated cells ($p > 0.001$; Figure 3D). This demonstrated that inhibition of PI3K is integral to the action of **1**. Experiments with Pi103 alone showed similar results (Figure S5).

We then examined the responsiveness of **1** to changes in ROS levels in Kasumi-1 cells (Figure 3D). Cells were treated with **1** at the IC_{50} value and co-treated with an antioxidant, 100 μM

glutathione (GSH), or oxidative stress inducers, hydrogen peroxide (100 μM) or 50 μM tert-butyl hydroperoxide (TBHP). Addition of **1** led to a reduction in cell viability as monitored by MTT to 55% ±5%. Treatments alone with hydrogen peroxide or tert-Butyl hydroperoxide showed modest reductions in viability. Treatment with glutathione alone led to a small increase in viability. Co-treatment led to the following effects. It was found that glutathione when added to **1** led to a reduction in the activity of **1** and an increase in viability to 75±6% ($p < 0.01$). This result is consistent with reduction in cellular ROS leading to lower release of Pi103 from **1**. Addition of hydrogen peroxide increased the activity of **1** and further reduced viability to 24± 3% ($p < 0.01$). Similar results are shown for tert-butyl hydroperoxide with viability being lowered to and 35±4%. These results are consistent with increased cellular ROS leading to more release of Pi103 from **1**. Furthermore, we synthesized a compound where the aniline nitrogen is replaced by a nitro functional group (compound **8** in SI, Figure S6). The nitro group is a strong electron withdrawer that will make oxidation harder and release of Pi103 lower. If activity is reduced by this compound, then the ROS-activation activity of **1** is essential for activation. In fact, compound **8** has activity reduced by more than 35-fold relative to **1**. Thus, self-cyclizing prodrug **1** is sensitive for the ROS changes in cells.

One clear problem with drug release induced by oxidation is that first pass metabolism will rapidly react with the self-cycling prodrug. We examined this effect by incubating **1** and Pi103 with human liver microsomes followed by analysis of the compound remaining overtime using HPLC. These microsomes are established models for first pass metabolism, and the literature indicates that Pi103 is unstable to liver microsomes.[38] Indeed, when we incubated Pi103 with liver microsomes, the half-life was 3±0.6 hours, whereas little degradation of **1** was observed after 6 hours (Figure 3E). Thus, the self-cycling prodrug enhances stability in the harsh liver environment.

We next wanted to examine activity of **1** under conditions of elevated ROS induced by a chemotherapeutic drug. In this study, we examined if **1** would synergize with cytosine arabinoside (Figure 4A) or doxorubicin (Figure 4B), standard AML chemotherapeutics that are known to generate ROS. We measured cell viability of Kasumi-1 and cord blood cells in the presence of either doxorubicin or cytosine arabinoside with and without 1 μM **1**. We chose a low concentration of **1** to highlight the synergism since this concentration will have little cytotoxicity on its own as **1** reduced viability by less than 12% alone in both cell lines. We then examined AraC alone. After 72 hours, 0.03 μM cytosine arabinoside alone reduced viability of Kasumi-1 cells to 90±5% of the vehicle-treated control; the same dose reduced viability of cord blood cells to 81±3% of the vehicle-treated control (Figure 4A). When both AraC and **1** were co-incubated viability was reduced to 39±2% in Kasumi-1 cells whereas the effect in cord blood cells was statistically insignificant. Similar experiments were accomplished with doxorubicin. When Kasumi-1 cells were treated with 3 nM doxorubicin and **1** viability was 27±3% compared to 75±4% in cells treated with doxorubicin alone (Figure 4B). Cord blood cell viability was not significantly different when cells were

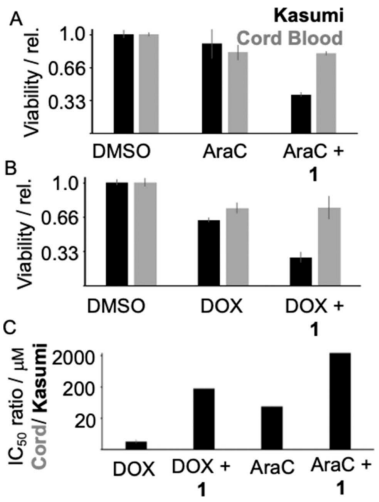

Figure 4. Compound **1** and AML chemotherapeutics act synergistically. A) Viability of Kasumi-1 cells (black bars) and cord blood cells (grey bars) in the presence of 30 nM cytosine arabinoside (AraC) with and without 1 μM **1** and B) in the presence of 3 nM doxorubicin (DOX) with and without 1 μM **1**. Viability is relative to DMSO-treated controls. C) Log ratios of IC_{50} values in the two cell lines for chemotherapeutics with and without **1**. All error bars are standard deviations form three biological replicates.

treated with a combination of either chemotherapeutic and **1** than when the cells were treated with chemotherapeutic alone (Figure 4B). These preliminary experiments suggest that **1** acts synergistically with the drugs cytosine arabinoside and doxorubicin.

To better understand the effect of the combination treatment, the IC_{50} values of the chemotherapeutic drugs were quantified in the presence of 1 μM **1** (Figure 4C). The IC_{50} of AML cells to that of the cord blood cells was 24±0.3 meaning that the IC_{50} value was 24-fold lower for AML cells. In the presence of **1** the ratio was 2222±80, which is an increase in selectivity of about 90-fold. For doxorubicin, the selectivity increased about 25-fold upon co-treatment with **1**. Most studies in PI3K inhibitors focus on synergism of proteins in the pathway.[39] Instead we show that the ROS production of commonly used agents can invoke strong synergy owing to the ROS-activatable self-cyclizing prodrug. Thus, **1** synergizes with chemotherapeutic compounds that induce ROS production, dramatically enhancing their selectivity for cancer cells relative to normal cells.

Conclusions

In this study, an oxidation prone chemical motif was attached to a PI3K inhibitor to create self-cycling prodrug **1** that undergoes a tandem reaction to release Pi103. The released Pi103 and self-cyclizing products were detected in cells after treatment. Importantly, the oxidation is slow, occurring over days. Prodrug **1** was selective for cells with high ROS or oxidative equivalents relative to normal cord blood cells. Strong synergistic effects were observed with chemotherapeutic drugs

that induce oxidative stress. This design can be adapted to other inhibitors and for conjugation to biomolecules. Previously evaluated PI3K inhibitors were detrimental to normal cell types resulting in serious side effects. Compound **1** warrants further testing as it has the benefits of acting synergistically with chemotherapeutics that induce ROS but with selectivity for cancerous cells.

Experimental Section

Synthesis

Pi103 was obtained from MedChem Express. All other chemicals were obtained from Fisher Scientific. NMR spectrum was generated at the Nuclear Magnetic Resonance Facility in Department of Chemistry, University of Cincinnati using Bruker AV 400 MHz spectrometer. Mass Spectrum was obtained at R. Marshall Wilson Mass Spectrometry Facility at University of Cincinnati.

Full synthetic details and spectra are within the supporting information including the synthesis of **1A**^{ox}, **1B**^{ox}, and 8. The following protocol was used to synthesize **1** as shown in Scheme 1.

Synthesis of 5-nitro-2-(3-(4-morpholinopyrido[3′,2′:4,5]-furo-[3,2-d] pyrimidin-2-yl)phenoxy)benzenamine (2). To a solution of 3-(4-morpholinopyrido[3′,2′:4,5]-furo-[3,2-d] pyrimidin-2-yl) phenol (50 mg, 0.15 mmol) in DMSO (2 mL), K_2CO_3 (30 mg, 0.2 mmol) was added, followed by addition of 2-fluoro-5-nitrobenzenamine (50 mg, 0.3 mmol). The resulting mixture was stirred at 70 °C overnight. After overnight incubation, the reaction mixture was diluted with 25 mL H_2O and extracted with ethyl acetate and washed with brine. The organic layer was dried with Na_2SO_4 and concentrated in vacuum. The resulting material was purified by flash chromatography using ethyl acetate/hexane (1:1) as eluent to generate the product as a yellowish solid [70 mg, 95%]. ^{1}H NMR (400 MHz, Chloroform-d) δ 8.62 (dd, J = 4.9, 1.8 Hz, 1H), 8.58 (dd, J = 7.7, 1.8 Hz, 1H), 8.32 (d, J = 7.8, 1H), 8.28(s,1H), 7.72 (d, J = 2.7 Hz, 1H), 7.58–7.52 (m, 2H), 7.43 (dd, J = 7.7, 4.8 Hz, 1H), 7.13–7.06 (m, 1H), 6.81 (d, J = 8.9 Hz, 1H), 4.27 (s, 2H), 4.22 (t, J = 4.8 Hz, 4H), 9.92 (t, J = 4.8 Hz, 4H). ^{13}C NMR (101 MHz, CDCl3) δ 162.70, 158.52, 155.22, 149.74, 148.81, 147.24, 143.55, 140.80, 137.91, 133.44, 131.86, 130.14, 124.74, 121.07, 120.34, 119.52, 115.90, 115.23, 114.32, 110.26, 66.89, 45.75. [M + H]: 485.1564

Synthesis of Benzyl-2-(5-nitro-2-(3-(4-morpholinopyrido [3′,2′:4,5]-furo-[3,2-d]pyrimidin-2-yl)phenoxy)phenylamino)-2-oxoethylcarbamate (3). To a room temperature (RT) solution of the 2-(benzyloxycarbonyl) acetic acid (100 mg, 0.5 mmol) in DMF (2.0 mL), Hexafluorophosphate Azabenzotriazole Tetramethyl Uronium (380 mg, 1 mmol) was added, then 5-nitro-2-(3-(4-morpholinopyrido[3′,2′:4,5]-furo-[3,2-d] pyrimidin-2-yl) phenoxy) benzene amine (**2**, 50 mg, 0.1 mmol) was added after 30 mins. Then N,N-diisopropylethylamine (0.36 mL, 0.2 mmol) was added. The resulting mixture was stirred at 40 °C for 24 h. The reaction was diluted with 25 mL H_2O and extracted with ethyl acetate, washed with brine. The organic layer was dried with Na_2SO_4 and concentrated in vacuum. The resulting material was purified by flash chromatography using ethyl acetate/hexane (1:1) and product was eluted as yellowish solid [30 mg, 40%]. ^{1}H NMR (400 MHz, Chloroform-d) δ 9.33 (s, 1H), 8.73(s,1H) 8.61 (d, J = 7.7 1H), 8.56 (dd, J = 7.7, 1.7 Hz, 1H), 8.42 (d, J = 7.9 Hz, 1H), 8.23 (s, 1H), 7.91 (dd, J = 9.1, 2.8 Hz, 1H), 7.57 (t, J = 7.9 Hz, 1H), 7.47 (dd, J = 7.7, 4.8 Hz, 1H), 6.88 (d, J = 9.1 Hz, 1H),6.83 (m,5H) 5.11 (d, J = 3.9 Hz, 2H), 4.21 (t, J = 4.8 Hz, 4H), 4.12 (d, J = 5.9 Hz, 2H), 3.91 (t, J = 4.8 Hz,4H).^{13}C NMR (101 MHz,CDCl3)δ167.70, 162.65, 158.14, 154.27, 151.59, 149.80, 148.80, 147.15, 142.09, 141.09, 135.75, 133.43, 131.86, 130.42, 128.55, 128.32, 128.08, 125.67, 121.69, 120.40, 120.01, 116.19, 115.10, 114.79, 67.56, 66.86, 45.72, 38.64. [M + H]:676.2147

Synthesis of 2-amino-N-(5-amino-2-(3-(4-morpholinopyrido [3′,2′:4,5]furo[3,2-d]pyrimidin-2-yl)phenoxy)phenyl)acetamide (1). To a room temperature (RT) solution of the benzyl 2-(5-nitro-2-(3-(4-morpholinopyrido[3′,2′:4,5]-furo-[3,2-d]pyrimidin-2-yl) phenoxy)phenylamino)-2-oxoethylcarbamate (**3**, 30 mg, 0.04 mmol) in MeOH (5.0 mL),10% Pd on carbon (4 mg) was added, and the solution purged with H_2 for 3 min. The pressure safe vial was sealed and allowed H_2 added until the pressure was 30 psi. The resulting mixture was stirred at RT for 24 hr. The reaction was filtered with Celite and concentrated in vacuum. The resulting material was purified by flash chromatography using DCM/MeOH (9:1) and product was eluted as yellowish solid [20 mg, 95%]. 1H NMR (400 MHz, DMSO-d6) δ 8.580–8.50 (m, 2H), 7.96 (d, J = 2.5 Hz, 1H), 7.63 (dd, J = 7.7, 4.8 Hz, 1H), 7.56–7.36 (m, 2H),7.31 (dd, J = 8.1, 2.4 Hz, 1H) 6.96 (dd, J = 8.1, 2.6 Hz, 1H), 6.76 (d, J = 8.6 Hz, 1H), 6.47 (dd, J = 8.8, 2.6 Hz, 1H), 4.01 (t, J = 4.8 Hz, 4H), 3.78 (t, J = 4.8 Hz, 4H) 3.21(s,2H). 13 C NMR (400 MHz, MeOHd6) δ163.78, 160.27, 150.80, 149.96, 147.97, 146.28, 141.02, 139.44, 135.32, 134.58, 133.32, 131.60, 130.66, 123.09, 122.67, 121.88, 119.56, 117.35, 116.21, 113.39, 110.81, 107.43, 67.85, 46.98, 38.89 [M + H] 512.2039.

Cell Assays

CD34+ selected Human Umbilical Cord Blood (UCB), HL60, Kasumi-1 and MOLM13 cell lines were generous gift from Dr. Mark Wunderlich at CCHMC. AML cells were cultured in IMDM media supplemented with 20% bovine calf serum. Human Umbilical Cord Blood (UCB) cells were cultured in IMDM media in 20% bovine calf serum supplemented with growth factors such as SCF, IL-3, IL-6, Flt-3L and TPO. NH-Fibroblast cells were culture in MDME media with 10% bovine calf serum and supplemented with growth factors such as Insulin, HC, EGF.

Cell Cytotoxicity Assay (MTT)

In all assays cells were seeded at a density of 0.4×10^6 cells/well in a 96-well plate and incubated at 37 °C overnight. Then cells were treated for 72 hr with indicated concentrations of freshly dissolved compounds. The plates were centrifuged at 1500Xg, washed, and each well was incubated for an additional 4 hr with 500 μL fresh medium containing 20 μL of MTT (5 mg/mL). Next, 100 μL of DMSO was added to each well and the optical densities (ODs) were determined at 570 nm using spectrophotometer. Cytotoxicity data were expressed as IC_{50} values obtained from the fit to a four-parameter sigmoid using graph pad prism 7 (GraphPad Software, Inc., La Jolla, CA). All R^2 values were greater than 0.98 and standard errors of the three replicates were less than 20%. All values are expressed as the mean of biological triplicates relative to DMSO control together with standard deviation shown as the error bar. The bar graph was generated using graph pad prism 7 (GraphPad Software, Inc., La Jolla, CA).

In Cell Western Blot Analysis

In this experiment, Kasumi-1 cells were grown in a 96-well non-treated plate and treated with different concentration of tested agents for 18 hr. The cells were counted and reset to 0.4×10^6 cells/mL. Then the experiment was performed using following steps. Step1: media was removed from wells and the cells were washed two times with 1X PBS. Step 2: 150 μL/well of 3.7% formaldehyde in PBS was added and incubated for 20 min at room temp without

shaking. Step 3: After aspiration and removal of fixing solution cells were permeabilized using 200 μL/well of 1X PBS in 0.1% Triton X-100 four times for 5 min each. Step 4. Each well was blocked by adding 150 μL/well of blocking buffer and washed (4X) using 200 μL/well PBS with 0.1% Tween-20. Step 5: Incubation (4 °C for overnight) of the primary antibody was accomplished by addition of 50 μL/well mouse anti-AKT primary antibody or rabbit anti-phospho AKT primary antibody. Both antibody solutions were 2.5 μg/mL (1:400). Step 6: After washing the secondary antibody, 50 μL/well anti-mouse IgG IRDye 800 or anti-rabbit IgG IRDye600 diluted 1:1000 times in blocking buffer, was added and incubated for 2 hr at RT with gentle shaking. Step 7: After washing the plate was dried and imaged using LI-COR odyssey infrared imager. Unpaired t-test was performed to determine the significance. Six biological replicates were used to obtain averages and standard deviations.

Quantification of In-Cell Release Experiment

Cells were seeded at a density of 0.4×10^6 cells/well in a 6-well plate and incubated at 37 °C overnight. Then the cells were treated for 24 and 72 hr using the indicated concentrations of freshly dissolved compounds (10 μM). The cells were transferred and centrifuged at 1500Xg and the media was removed. Then the cells were treated with 0.1% formic acid in acetonitrile for 30 min at 4 °C and centrifuged at 1500Xg. The organic layer was filtered and analyzed using HPLC. Four biological replicates were performed.

Liver Microsome PK Study

To a 1.7 mL eppendorf tube, 1.35 mL buffer [50 mM phosphate buffer (pH 7.4), 1 mM EDTA pH 8, 3 mM $MgCl_2$, 0.25 mM NADPH, pH 7.4] and 0.15 mL sample [5 mM with 0.5% DMSO] was added at 37 °C . Then, 4 μL 0.1 mg/mL human liver microsomes were added to the above mixture. At the time points a 150 μL aliquot of reaction mix added to 150μL of acetonitrile in a plastic HPLC vial and centrifuged. 100 μL was filtered through a 20 micron filter and 25 μL injected onto the HPLC equipped with an Agela Vensil column (4.6 ID, 100 mm, 3 μm particles) and separated by a gradient that ranged from 5% acetonitrile to 90% acetonitrile in water with 0.1% formic acid. Chromatograms were integrated and plotted over time. Data points represent three biological replicates.

Acknowledgements

This study was supported by Department of Defense grant W81XWH-16-1-0489 and 1R15ES029675 to EJM, University of Cincinnati Collaborative Advancement Grants Program Strategic Teams to EJM and JTG. Mass Spectrometry was enabled by NSF award number 1828072 to EJM. In addition, support by CA181347 to JTG and EJM is acknowledged. In addition, the undergraduate researchers were funded by NSF research experience for undergraduates (1659648).

Conflict of Interest

The authors declare no conflict of interest.

Keywords: oxidative cyclization · phosphoinositide 3-kinase inhibitors · reactive oxygen species · synergy effects · prodrugs

[1] J. E. Burke, *Mol. Cell* **2018**, *71*, 653–673.
[2] E. C. Lien, C. C. Dibble, A. Toker, *Curr. Opin. Cell Biol.* **2017**, *45*, 62–71.
[3] M. D. Goncalves, B. D. Hopkins, L. C. Cantley, *N. Engl. J. Med.* **2018**, *379*, 2052–2062.
[4] D. A. Fruman, H. Chiu, B. D. Hopkins, S. Bagrodia, L. C. Cantley, R. T. Abraham, *Cell* **2017**, *170*, 605–635.
[5] P. Castel, H. Ellis, R. Bago, E. Toska, P. Razavi, F. J. Carmona, S. Kannan, C. S. Verma, M. Dickler, S. Chandarlapaty, E. Brogi, D. R. Alessi, J. Baselga, M. Scaltriti, *Cancer Cell* **2016**, *30*, 229–242.
[6] I. Galvao, C. M. Queiroz-Junior, V. L. Oliveira, V. Pinho Da Silva, E. Hirsch, M. M. Teixeira, *Front. Pharmacol.* **2018**, *9*, 1505.
[7] S. Matsuda, Y. Nakagawa, A. Tsuji, Y. Kitagishi, A. Nakanishi, T. Murai, *Diseases* **2018**, *6*, 28.
[8] N. N. Pavlova, C. B. Thompson, *Cell Metab.* **2016**, *23*, 27–47.
[9] Q. W. Fan, Z. A. Knight, D. D. Goldenberg, W. Yu, K. E. Mostov, D. Stokoe, K. M. Shokat, W. A. Weiss, *WA. Cancer Cell.* **2006**, *9*, 341–349.
[10] M. Lopez-Fauqued, R. Gil, J. Grueso, J. Hernandez-Losa, A. Pujol, T. Moline, J. A. Recio, *Int. J. Cancer* **2010**, *126*, 1549–1561.
[11] L. Tentori, P. M. Lacal, G. Graziani, *Trends Pharmacol. Sci.* **2013**, *34*, 656–666.
[12] J. N. Moloney, T. G. Cotter, *Semin. Cell Dev. Biol.* **2018**, *80*, 50–64.
[13] J. P. Cadahía, V. Previtali, N. S. Troelsen, M. H. Clausen, *MedChemComm* **2019**, *10*, 1531–1549.
[14] A. R. Jones, T. R. Bell-Horwath, G. Li, S. M. Rollmann, E. J. Merino, *Chem. Res. Toxicol.* **2012**, *25*, 2542–2552
[15] J. Liu, H. Zhu, G. Premnauth, K. G. Earnest, P. Hahn, G. Gray, J. A. Queenan, L. E. Prevette, S. F. AbdulSalam, A. L. Kadekaro, *Free Radical Biol. Med.* **2019**, *134*, 133–138.
[16] S. Toyokuni, F. Ito, K. Yamashita, Y. Okazaki, S. Akatsuka, *Free Radical Biol. Med.* **2017**, *108*, 610–626.
[17] C. Gorrini, I. S. Harris, T. W. Mak, *Nat. Rev. Drug Discovery* **2013**, *12*, 931–947.
[18] M. Nieborowska-Skorska, S. Flis, T. Skorski, *Leukemia* **2014**, *28*, 2416–2418.
[19] Y. M. Hu, W. Q. Lu, G. Chen, P. Wang, Z. Chen, Y. Zhou, M. Ogasawara, D. Trachootham, L. Feng, H. Pelicano, P. J. Chiao, M. J. Keating, G. Garcia-Manero, P. Huang, *Cell Research* **2012**, *22*, 399–412.
[20] M. E. Irwin, N. Rivera-Del Valle, J. Chandra, *Antioxid. Redox Signaling* **2013**, *18*, 1349–1383.
[21] S. F. Abdul Salam, P. N. Gurjar, H. Zhu, J. Liu, E. S. Johnson, A. L. Kadekaro, J. Landero-Figueroa, E. J. Merino, *ChemBioChem* **2017**, *18*, 2007–2011.
[22] A. K. Vadukoot, S. F. Abdul Salam, M. Wunderlich, E. D. Pullen, J. Landero-Figueroa, J. C. Mulloy, E. J. Merino, *Bioorg. Med. Chem.* **2014**, *22*, 6885–6892.
[23] B. Kalyanaraman, G. Cheng, M. Hardy, O. Ouari, B. Bennett, J. Zielonka, *Redox Biology* **2018**, *15*, 347–362.
[24] T. T. Hoang, T. P. Smith, R. T. Raines, *Angew. Chem. Int. Ed.* **2017**, *56*, 2619–2622; *Angew. Chem.* **2017**, *129*, 2663–2666.
[25] Y. Liao, L. P. Xu, S. Y. Ou, H. Edwards, D. Luedtke, Y. B. Ge, Z. H. Qin, *ACS Med. Chem. Lett.* **2018**, *9*, 635–640.
[26] S. D. Bhagat, U. Singh, R. K. Mishra, A. Srivastava, *ChemMedChem.* **2019**, *13*, 2073–2079.
[27] K. Matsushita, T. Okuda, S. Mori, M. Konno, H. Eguchi, A. Asai, J. Koseki, Y. Iwagami, D. Yamada, H. Akita, T. Asaoka, *ChemMedChem.* **2019**, *14*, 1384–1391.
[28] R. D. Hanna, Y. Naro, A. Deiters, P. E. Floreancig, *J. Am. Chem. Soc.* **2016**, *138*, 13353–13360.
[29] M. A. Soriano-Ursúa, E. D. Farfán-García, Y. López-Cabrera, E. Querejeta, J. G. Trujillo-Ferrara, *Neurotoxicology* **2014**, *40*, 8–15.
[30] E. D. Farfán-García, N. T. Castillo-Mendieta, F. J. Ciprés-Flores, I. I. Padilla-Martínez, J. G. Trujillo-Ferrara, M. A. Soriano-Ursúa, *Toxicol. Lett.* **2016**, *258*, 115–125.
[31] S. J. Baker, C. Z. Ding, T. Akama, Y. K. Zhang, V. Hernandez, Y. Xia, *Future Med. Chem.* **2009**, *1*, 1275–1288.
[32] Y. L. Zhao, X. Zhang, Y. Y. Chen, S. Y. Lu, Y. F. Peng, X. Wang, C. L. Guo, A. W. Zhou, J. M. Zhang, Y. Luo, Q. C. Shen, J. Ding, L. H. Meng, J. Zhang, *ACS Med. Chem. Lett.* **2014**, *5*, 138–142.

[33] M. Hayakawa, H. Kaizawa, H. Moritomo, T. Koizumi, T. Ohishi, M. Yamano, M. Okada, M. Ohta, S. I. Tsukamoto, F. I. Raynaud, *Bioorg. Med. Chem. Lett.* **2007**, *17*, 2438–2442.
[34] B. W. Jester, K. J. Cox, A. Gaj, C. D. Shomin, J. R. Porter, I. Ghosh, *J. Am. Chem. Soc.* **2010**, *132*, 11727–11735.
[35] L. Larizza, I. Magnani, A. Beghini, *Leuk. Lymphoma* **2005**, *46*, 247–255.
[36] B. D. Manning, A. Toker, *Cell*, *169*, 381–405.
[37] J. P. Lai, J. Dalton, D. Knoell, *Br. J. Pharmacol.* **2007**, *152*, 1172–1184.
[38] F. I. Raynaud, S. Eccles, P. A. Clarke, A. Hayes, B. Nutley, S. Alix, A. Henley, F. Di-Stefano, Z. Ahmad, S. Guillard, L. M. Bjerke, L. Kelland, M. Valenti, L. Patterson, S. Gowan, A. de Haven Brandon, M. Hayakawa, H. Kaizawa, T. Koizumi, T. Ohishi, S. Patel, N. Saghir, P. Parker, M. Waterfield, P. Workman, *Cancer Res.* **2007**, *67*, 5840–5850.
[39] E. Pons-Tostivint, B. Thibault, J. Guillermet-Guibert, *Trends Cancer* **2017**, *3*, 454–469.

Manuscript received: August 19, 2019
Revised manuscript received: October 3, 2019
Version of record online: ■■, ■■■

FULL PAPERS

Super selectivity: We designed a self-cyclizing prodrug that is activated with cellular oxidation, leading to ether cleavage. The slow release is increased by external stressors leading to release of a PI3K inhibitor. We show experiments proving the mechanism and exceptional synergy with common anticancer agents.

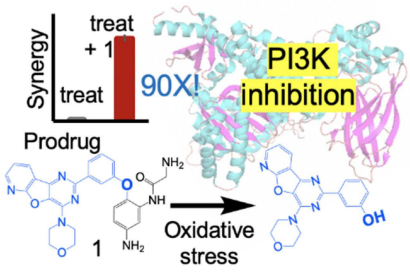

*H. Zhu, Dr. R. Mishra, L. Yuan, S. F. Abdul Salam, J. Liu, G. Gray, A. D. Sterling, Dr. M. Wunderlich, Prof. Dr. J. Landero-Figueroa, Dr. J. T. Garrett, Prof. Dr. E. J. Merino**